Active Inference for Fault Tolerant Control of Robot Manipulators with Sensory Faults

Corrado Pezzato[1], Mohamed Baioumy[3], Carlos Hernández Corbato[1], Nick Hawes[3], Martijn Wisse[1], and Riccardo Ferrari[2]

[1] Cognitive Robotics, Delft University of Technology
[2] Delft Center for Systems and Control, Delft University of Technology
{c.pezzato, c.h.corbato, r.ferrari, m.wisse}@tudelft.nl
[3] Oxford Robotics Institute, University of Oxford
{mohamed, nickh}@robots.ox.ac.uk

Abstract. We present a fault tolerant control scheme for robot manipulators based on active inference. The proposed solution makes use of the sensory prediction errors in the free-energy to simplify the residuals and thresholds generation for fault detection and isolation and does not require additional controllers for fault recovery. Results validating the benefits in a simulated 2DOF manipulator are presented and the limitations of the current approach are highlighted.

Keywords: Fault-tolerant control · fault recovery · active inference · free-energy · robot manipulator

1 Introduction

Developing fault tolerant (FT) control schemes is of vital importance to bring robots outside controlled laboratories. The area of fault tolerant control has become increasingly more important in recent years, and several methods have been developed in different fields. An extensive bibliographical review and classification of FT methods can be found in [25]. Model-based FT techniques are amongst the most promising approaches [8]. For fault detection, they rely on mathematical models to generate *residual* signals to be compared to a *threshold*. Fault recovery is then often performed by switching among different available fault-specific controllers [17]. The two main challenges to design FT schemes are the definition of residuals and thresholds, and the design of a fault specific recovery strategy. We present a novel FT scheme for sensory faults [19, 23] based on an active inference controller (AIC) [20], which is inspired by the active inference framework. Active inference is prominent in the neuroscientific literature as a general theory of the brain [9–11] and several recent approaches in robotics have taken inspiration from it [1–3, 15, 16, 18, 20–22, 24]. In this work we investigate the utility of the active inference framework for fault-tolerant control with sensory faults. In the presented scheme, we exploit the properties of the framework to simplify the definition of both residuals and thresholds, and we provide a simple and general mechanism for sensory fault recovery. Our approach is validated on a simulated 2DOF manipulator.

2 Problem statement

We consider a robot controlled in joint space with torque commands, using an active inference controller (AIC) [20, 1]. In the following, we highlight the necessary elements and assumptions to derive an expression for the free-energy of the system, and the equations for state estimation and control. This study considers a 2-DOF robot arm, equipped with a vision system to retrieve the end effector Cartesian position $\boldsymbol{y}_v = [y_{v_x},\ y_{v_z}]^\top$, and with position and velocity sensors $\boldsymbol{y}_q,\ \boldsymbol{y}_{\dot{q}} \in \mathbb{R}^2$ for the two joints. Thus, we define $\boldsymbol{y} = [\boldsymbol{y}_q,\ \boldsymbol{y}_{\dot{q}},\ \boldsymbol{y}_v]$. The

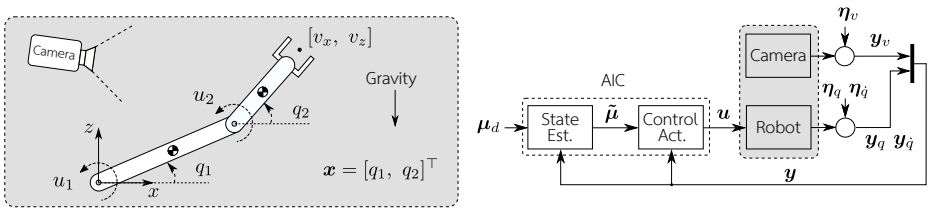

Fig. 1. 2-DOF robot arm and general AIC control scheme.

proprioceptive sensors and the camera are affected by zero mean Gaussian noise $\boldsymbol{\eta} = [\boldsymbol{\eta}_q,\ \boldsymbol{\eta}_{\dot{q}},\ \boldsymbol{\eta}_v]$. Additionally, the camera is affected by barrel distortion. The states $\boldsymbol{x}$ to be controlled are set as the joint positions $\boldsymbol{q}$ of the robot arm. We define the generative model of the state dynamics $\boldsymbol{f}(\cdot)$ such that the robot will be steered to a desired joint configuration $\boldsymbol{\mu}_d$ following the dynamics of a first order linear system with time constant τ.

$$\boldsymbol{f}(\boldsymbol{\mu}) = (\boldsymbol{\mu}_d - \boldsymbol{\mu})\tau^{-1} \tag{1}$$

The relation between $\boldsymbol{\mu}$ and $\boldsymbol{y}$ is expressed through the generative model of the sensory input $\boldsymbol{g} = [\boldsymbol{g}_q,\ \boldsymbol{g}_{\dot{q}},\ \boldsymbol{g}_v]$. Since we set $\boldsymbol{x} = [q_1,\ q_2]^\top$ and we can directly measure joint positions, $\boldsymbol{g}_q$ and $\boldsymbol{g}_{\dot{q}}$ and their partial derivatives are [20, 7]:

$$\boldsymbol{g}_q(\boldsymbol{\mu}) = \boldsymbol{\mu}, \quad \boldsymbol{g}_{\dot{q}}(\boldsymbol{\mu}) = \boldsymbol{\mu}', \quad \partial \boldsymbol{g}_q(\boldsymbol{\mu})/\partial \boldsymbol{\mu} = 1, \quad \partial \boldsymbol{g}_{\dot{q}}(\boldsymbol{\mu})/\partial \boldsymbol{\mu}' = 1 \tag{2}$$

Note that $\boldsymbol{\mu}'$ is the first order generalised motion of $\boldsymbol{\mu}$. To define $\boldsymbol{g}_v(\boldsymbol{\mu})$, instead, we use a *Gaussian Process Regression* (GPR) as in [16]. The training data is composed by a set of observations of the camera output $[\bar{\boldsymbol{y}}_{v_x},\ \bar{\boldsymbol{y}}_{v_z}]^\top$ in several robot configurations $\bar{\boldsymbol{y}}_q$. We use a squared exponential kernel k of the form:

$$k(\boldsymbol{y}_{q_i}, \boldsymbol{y}_{q_j}) = \sigma_f^2 \exp\left(-\tfrac{1}{2}(\boldsymbol{y}_{q_i} - \boldsymbol{y}_{q_j})^\top \Lambda (\boldsymbol{y}_{q_i} - \boldsymbol{y}_{q_j})\right) + \sigma_n^2 d_{ij}$$

where $\boldsymbol{y}_{q_i},\ \boldsymbol{y}_{q_j} \in \bar{\boldsymbol{y}}_q$, and d_{ij} is the Kronecker delta function. Λ is a diagonal matrix of hyperparameters to be optimised. It holds then:

$$\boldsymbol{g}_v(\boldsymbol{y}_{\boldsymbol{q}*}) = \begin{bmatrix} K_* K^{-1} \bar{\boldsymbol{y}}_{v_x} \\ K_* K^{-1} \bar{\boldsymbol{y}}_{v_z} \end{bmatrix} \quad \boldsymbol{g}_v(\boldsymbol{y}_{\boldsymbol{q}*})' = \begin{bmatrix} -\Lambda^{-1}(\boldsymbol{y}_{\boldsymbol{q}*} - \bar{\boldsymbol{y}}_q)^\top [k(\boldsymbol{y}_{\boldsymbol{q}*}, \bar{\boldsymbol{y}}_q)^\top \cdot \boldsymbol{\alpha}_x] \\ -\Lambda^{-1}(\boldsymbol{y}_{\boldsymbol{q}*} - \bar{\boldsymbol{y}}_q)^\top [k(\boldsymbol{y}_{\boldsymbol{q}*}, \bar{\boldsymbol{y}}_q)^\top \cdot \boldsymbol{\alpha}_z] \end{bmatrix} \tag{3}$$

where $\cdot$ means element-wise multiplication, $\boldsymbol{\alpha}_x = K^{-1}\bar{\boldsymbol{y}}_{v_x}$ and $\boldsymbol{\alpha}_z = K^{-1}\bar{\boldsymbol{y}}_{v_z}$, with K being the covariance matrix.

Given the generative models $\boldsymbol{f}$ and $\boldsymbol{g}$ as before, we can define an expression for the free-energy $\mathcal{F}$. Under Laplace approximation, and considering normally distributed uncorrelated noise and generalised motions up to second order, the free-energy for the 2-DOF robot arm can be expressed as:

$$\mathcal{F} = \frac{1}{2}\sum_i \left(\boldsymbol{\varepsilon}_i^\top P_i \boldsymbol{\varepsilon}_i + \ln|P_i|\right) + C, \qquad i \in \{y_q,\ y_{\dot{q}},\ y_v,\ \mu,\ \mu'\} \tag{4}$$

where and C is a constant and P_i defines a precision (or inverse covariance) matrix. Note that we set $\tau = 1$ as in [20]. The terms $\boldsymbol{\varepsilon}_i = (\boldsymbol{y}_i - \boldsymbol{g}_i(\mu))$ with $i \in \{y_q,\ y_{\dot{q}},\ y_v\}$ are the *Sensory Prediction Errors* (SPE), representing the difference between observed sensory input and expected one. The model prediction errors are instead defined considering the desired state dynamics as $\boldsymbol{\varepsilon}_\mu = (\boldsymbol{\mu}' - \boldsymbol{f}(\mu))$ and $\boldsymbol{\varepsilon}_{\mu'} = (\boldsymbol{\mu}'' - {}^{\partial \boldsymbol{f}(\mu)}/_{\partial \boldsymbol{\mu}\mu'})$. In particular, for the 2-DOF example it results that $\boldsymbol{\varepsilon}_q = (\boldsymbol{y}_q - \boldsymbol{\mu})$, $\boldsymbol{\varepsilon}_{\dot{q}} = (\boldsymbol{y}_{\dot{q}} - \boldsymbol{\mu}')$, $\boldsymbol{\varepsilon}_v = (\boldsymbol{y}_v - \boldsymbol{g}_{\boldsymbol{v}}(\boldsymbol{\mu}))$, and $\boldsymbol{\varepsilon}_\mu = (\boldsymbol{\mu}' + \boldsymbol{\mu} - \boldsymbol{\mu}_d)$, $\boldsymbol{\varepsilon}_{\mu'} = (\boldsymbol{\mu}'' + \boldsymbol{\mu}')$. For more details on the derivation of equation (4), an interested reader can refer to [20, 6, 7].

Finally, one can compute the generalised state estimates $\boldsymbol{\mu}$, $\boldsymbol{\mu}'$, and $\boldsymbol{\mu}''$, and control actions $\boldsymbol{u}$ by minimizing $\mathcal{F}$ through gradient descent [11]:

$$\dot{\boldsymbol{\mu}} = \boldsymbol{\mu}' - \kappa_\mu \frac{\partial \mathcal{F}}{\partial \boldsymbol{\mu}}, \qquad \dot{\boldsymbol{\mu}}' = \boldsymbol{\mu}'' - \kappa_\mu \frac{\partial \mathcal{F}}{\partial \boldsymbol{\mu}'}, \qquad \dot{\boldsymbol{\mu}}'' = -\kappa_\mu \frac{\partial \mathcal{F}}{\partial \boldsymbol{\mu}''} \tag{5}$$

$$\dot{\boldsymbol{u}} = -\kappa_a \frac{\partial \boldsymbol{y}_q}{\partial \boldsymbol{u}} P_{y_q}(\boldsymbol{y}_q - \boldsymbol{\mu}) - \kappa_a \frac{\partial \boldsymbol{y}_{\dot{q}}}{\partial \boldsymbol{u}} P_{y_{\dot{q}}}(\boldsymbol{y}_{\dot{q}} - \boldsymbol{\mu}') - \kappa_a \frac{\partial \boldsymbol{y}_v}{\partial \boldsymbol{u}} P_{y_v}(\boldsymbol{y}_v - \boldsymbol{g}_v(\boldsymbol{\mu})) \tag{6}$$

Note that P_{y_q}, $P_{y_{\dot{q}}}$ and P_{y_v} are the precision matrices representing the confidence about sensory inputs. The higher the confidence in a sensor, the more reliable its measurements are assumed to be. Following [18, 20], we set $\partial \boldsymbol{y}_q/\partial \boldsymbol{u}$ and $\partial \boldsymbol{y}_{\dot{q}}/\partial \boldsymbol{u}$ to the identity, approximating the true relationships with only their sign. Similar considerations can be made for the relation between commanded torques and Cartesian displacements. The sign of $\partial \boldsymbol{y}_v/\partial \boldsymbol{u}$ depends on the combination of the two joint angles. For instance, operating the end effector in the fourth quadrant with $-\pi/2 \leq q_1 \leq 0$, a positive u_1 will lead to positive increments of both x and z coordinates. More advanced methods to determine these partial derivatives are out of the scope of this work, but definitely possible and encouraged.

3 A fault tolerant scheme based on active inference

In this section we define a fault tolerant scheme as in Fig. 2, using the SPE to build residuals for fault detection. We also show how the sensory redundancy and precision matrices can be used for fault recovery, such that we do not need to generate extra signals for detection as in conventional approaches, and we simplify fault recovery.

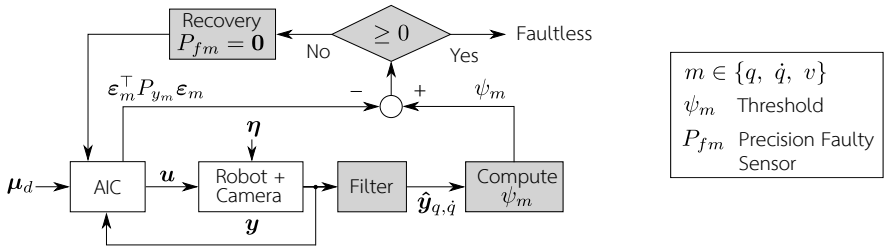

Fig. 2. AIC with additional elements (in gray) for fault tolerant control.

Threshold for fault detection and isolation (FDI) Even though the SPE can be seen as residuals for fault detection purposes, there is a substantial difference. In active inference, the belief $\boldsymbol{\mu}$ is biased towards a given goal, so the SPE can also increase for causes which are not related to sensory faults (i.e. the robot is stuck due to a collision). This precludes the use of established fault detection techniques to define a threshold ψ_m for FDI. To solve this issue we consider the quadratic form $\boldsymbol{\varepsilon}_m^\top P_{y_m} \boldsymbol{\varepsilon}_m$, where $\boldsymbol{\varepsilon}_m = \boldsymbol{y}_m - \boldsymbol{g}_m(\boldsymbol{\mu})$ with $m \in \{q,\ \dot{q},\ v\}$. The core idea is to compute an upper bound on this quadratic term. The first step is to compute an estimate for the prediction errors using the generative model as $\hat{\boldsymbol{\varepsilon}}_m = \boldsymbol{g}_m(\hat{\boldsymbol{x}}) - \boldsymbol{g}_m(\boldsymbol{\mu})$. The estimate of the joint positions $\hat{\boldsymbol{x}}$ is obtained through a filter using position and velocity measurements. Defining $\dot{\boldsymbol{x}} = \boldsymbol{z}$, we can write:

$$\dot{\hat{\boldsymbol{x}}} = \hat{\boldsymbol{z}} + H_1(\boldsymbol{y}_q - \hat{\boldsymbol{x}}) \qquad \dot{\hat{\boldsymbol{z}}} = H_2(\boldsymbol{y}_{\dot{q}} - \hat{\boldsymbol{z}}) \tag{7}$$

where $H_1,\ H_2$ are diagonal positive definite matrices. The estimation error can be made arbitrary small by choosing high gains H_1 and H_2 [12].

We can represent the sensory input $\boldsymbol{y}$ as a function of the ground truth $\boldsymbol{x}$ as:

$$\boldsymbol{y} = \boldsymbol{g}(\boldsymbol{x}) + \boldsymbol{\gamma} + \boldsymbol{\eta}\,, \tag{8}$$

where $\boldsymbol{\gamma} \in \mathbb{R}^6$ is a vector representing the process uncertainties introduced by the generative models $\boldsymbol{g}$, and $\boldsymbol{\eta}$ is the measurement noise. The sensory prediction error for a generic sensor m can then be written as:

$$\boldsymbol{\varepsilon}_m = \hat{\boldsymbol{\varepsilon}}_m + \underbrace{\boldsymbol{g}_m(\boldsymbol{x}) - \boldsymbol{g}_m(\hat{\boldsymbol{x}}) + \boldsymbol{\gamma}_m + \boldsymbol{\eta}_m}_{\boldsymbol{\delta}_m} = \hat{\boldsymbol{\varepsilon}}_m + \boldsymbol{\delta}_m \tag{9}$$

where $\boldsymbol{\delta}_m$ is the total uncertainty including process and measurement noise. The j-th entry $\delta_m(j)$ is a scalar total uncertainty associated with a specific sensor. Since we operate the robot in a finite workspace, with specific physical limits, the states of the system $\boldsymbol{x}$, the sensory input $\boldsymbol{y}$ and the internal belief $\boldsymbol{\mu}$ remain bounded in a compact region $\mathcal{R} = \mathcal{R}_x \times \mathcal{R}_y \times \mathcal{R}_\mu \subset \mathbb{R}^2 \times \mathbb{R}^6 \times \mathbb{R}^2$, before and after the occurrence of a fault. We also suppose that the noise $\boldsymbol{\eta}$ affecting the position and velocity sensors, and the camera, can be bounded. This means $||\boldsymbol{\eta}(t)||_2 \leq \bar{\boldsymbol{\eta}}$, where $\bar{\boldsymbol{\eta}}$ is a known value. Since the AIC does not require the full dynamical model of the robot arm, the characterization of the model uncertainties $\boldsymbol{\gamma}$ due

to $\boldsymbol{g}(\cdot)$ is straightforward: $\boldsymbol{g}_q(\cdot)$ and $\boldsymbol{g}_{\dot{q}}(\cdot)$ are just an identity, so no uncertainty is introduced, while for $\boldsymbol{g}_v(\cdot)$ we can retrieve the model uncertainty from the covariance matrix of the GPR. The sensory prediction errors $\boldsymbol{\varepsilon}_m$ and $\hat{\boldsymbol{\varepsilon}}_m$ are then bounded quantities, thus we can define an upper bound for the quadratic term $\boldsymbol{\varepsilon}_m^\top P_{y_m} \boldsymbol{\varepsilon}_m$.

Definition 1. *Given a maximum uncertainty $\bar{\boldsymbol{\delta}}_m$ such that $|\delta_m(j)| \leq \bar{\delta}_m(j)\ \forall j$, we define a threshold for fault detection for sensor m as:*

$$\psi_m = \hat{\boldsymbol{\varepsilon}}_m^\top P_{y_m} \hat{\boldsymbol{\varepsilon}}_m + 2|\hat{\boldsymbol{\varepsilon}}_{y_m}^\top P_{y_m} \bar{\boldsymbol{\delta}}_m| + \bar{\boldsymbol{\delta}}_m^\top P_{y_m} \bar{\boldsymbol{\delta}}_m \tag{10}$$

Lemma 1. *In a faultless case, the quadratic form of the sensory prediction errors for a sensor m will remain below the threshold ψ_m:*

$$\boldsymbol{\varepsilon}_m^\top P_{y_m} \boldsymbol{\varepsilon}_m \leq \psi_m \tag{11}$$

Proof. Once $\bar{\boldsymbol{\delta}}_m$ is given, and since P_{y_m} is diagonal positive definite, equation (11) follows from applying the triangular inequality, considering $\boldsymbol{\varepsilon}_m$ as in equation (9).

Using *Lemma 1*, a fault in a generic sensor m is detected and isolated whenever equation (11) is violated, that is when a fault will produce an anomaly in the sensory input bigger than $\bar{\boldsymbol{\delta}}_m$. The value for the maximum uncertainty is chosen according to the standard deviation of the noise present in the sensors. Note that, in theory, a bound $\bar{\boldsymbol{\eta}}$ may not be finite or could be very large making fault detection difficult or even impossible. In practice, using multiples of the variance, we reach an acceptable compromise between false alarms and detectability. Thus, each entry of $\bar{\boldsymbol{\delta}}_m$ is set to $5\sigma_m$ where $\boldsymbol{\eta}_m \sim \mathcal{N}(0, \sigma_m^2 I)$. Doing so, the probability of having a false alarm due to the noise is less that 10^{-6}.

Fault recovery To recover from a fault we exploit the fact that the controller encodes the precision matrices P_{y_q}, $P_{y_{\dot{q}}}$ and P_{y_v}. Once a fault is detected and isolated, fault recovery can be implemented simply by setting the precision matrix of the faulty sensor to zero, that is $P_{fm} = \mathbf{0}$. This is a simple and generic mechanism to recover for any kind of sensory fault once detected.

4 Simulation results

We control the robot from the initial position $\boldsymbol{q} = [-\pi/2,\ 0]$ (rad) to the desired position $\boldsymbol{\mu}_d = [-0.6,\ 0.5]$ (rad). A fault is injected either in the encoders or in the camera during the motion of the robot, at time $t_f = 2$ (s). The maximum uncertainties are set to $\bar{\boldsymbol{\delta}}_q = [5\sigma_q,\ 5\sigma_q]^\top$ and $\bar{\boldsymbol{\delta}}_v = [5\sigma_v,\ 5\sigma_v]^\top$, where $\sigma_q = 0.001$ and $\sigma_v = 0.01$. Figure 3A reports the single normalised SPE $\varepsilon_m^\top \sigma_m^{-1} \varepsilon_m / \psi_m$, that we call $N\varepsilon_m$. Doing so, a fault is detected when the ratio is bigger than one. We assume two kinds of possible faults: 1) A fault in the encoders: the output related to the first joint freezes so $\boldsymbol{y}_q(t) = [q_1(t_f),\ q_2(t)]^\top + \boldsymbol{\eta}_q$ for $t \geq t_f$, and 2) A fault

in the camera: a misalignment is injected as bias in $\boldsymbol{y}_v$. Figure 3A shows fault detection and isolation at t_{DI}, when the normalised residual is bigger than 1. The recovered and non-recovered response of the robot in case of encoder fault is depicted in Fig. 3B. A similar response is found for camera faults.

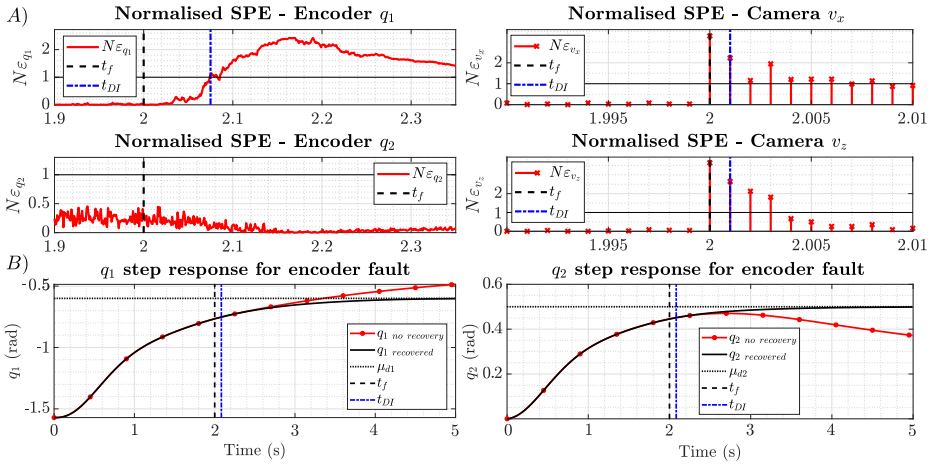

Fig. 3. A) Normalised SPE for FDI in case of encoder fault (left) or camera fault (right). B) Step response with and without recovery action in case of encoder fault.

5 Discussion and conclusion

Consider now equation (1). The time constant τ influences the generative model of the state dynamics $\boldsymbol{f}(\cdot)$, so the desired evolution of the states. As explained in [1], the AIC has two extremes depending on the value of τ^{-1} in the generative model. If $\tau^{-1} \to 0$, the estimation step has zero bias towards the target. The control action in this case will never steer the system towards the target. On the other hand, if $\tau^{-1} \to \infty$ the system is completely biased towards the target. That case is equivalent to a PID controller [1, 4, 5]. For any value in between, there is a compromise between estimation and control. The estimation and control are thus 'coupled'. This has a few limitations. First, the actions are not explicit in the model, so only sensory faults can be detected, isolated, and recovered. Second, the estimated state is always biased towards the desired state. Finally, biasing the state hinders learning model (hyper-)parameters.

What does this mean for the FT scheme presented so far? The bias could increase the SPE for reasons unrelated to sensory faults, for instance if the current target state changes to another which is further away from the current position. This prevents the direct use of the SPE as residuals in combination with established fault detection techniques, since it would cause several false positives.

It would then be beneficial to decouple estimation and control. In addition, a decoupled system could facilitate learning the hyperparameters. This could allow us to optimise the precision matrices for the SPE instead of setting P_{fm} to zero, since the precision matrices would represent the physical noise affecting the sensors. Decoupling can also help relaxing the assumption on the maximum $\bar{\boldsymbol{\delta}}_m$ which now has to be known a priori for the determination of the fault detection threshold. Approaches where the estimation and control are decoupled (similar to [3, 13, 14, 24]) for fault tolerance will be explored in future work.

To conclude, in this paper we present a novel approach for FT control based on active inference. The main novelty is the definition of an on-line threshold for FDI based on the SPE defined in the free-energy. Fault recovery is achieved by reducing the precision of faulty sensor to zero, providing a generic recovery mechanism which significantly simplifies the synthesis of reliable FT controllers. The main limitation of the proposed approach is that only sensory faults can be detected and recovered. Simulation results validated the theoretical findings. Future work will explore FT control with decoupled state-estimation and control.

References

1. Baioumy, M., Duckworth, P., Lacerda, B., Hawes, N.: Active inference for integrated state-estimation, control, and learning. arXiv preprint arXiv:2005.05894 (2020)
2. Baioumy, M., Mattamala, M., Duckworth, P., Lacerda, B., Hawes, N.: Adaptive manipulator control using active inference with precision learning. In: UKRAS (2020)
3. Baioumy, M., Mattamala, M., Hawes, N.: Variational inference for predictive and reactive controllers. In: ICRA 2020 Workshop on New advances in Brain-inspired Perception, Interaction and Learning. Paris, France (2020)
4. Baltieri, M., Buckley, C.L.: A probabilistic interpretation of pid controllers using active inference. In: International Conference on Simulation of Adaptive Behavior. pp. 15–26. Springer (2018)
5. Baltieri, M., Buckley, C.L.: Pid control as a process of active inference with linear generative models. Entropy **21**(3), 257 (2019)
6. Bogacz, R.: A tutorial on the free-energy framework for modelling perception and learning. Journal of mathematical psychology **76**, 198–211 (2017)
7. Buckley, C.L., Kim, C.S., McGregor, S., Seth, A.K.: The free energy principle for action and perception: A mathematical review. Journal of Mathematical Psychology **81**, 55–79 (2017)
8. Chen, J., Patton, R.J.: Robust model-based fault diagnosis for dynamic systems. Springer Science & Business Media, LLC (1999)
9. Friston, K.J.: The free-energy principle: a unified brain theory? Nature Reviews Neuroscience **11(2)**, 27–138 (2010)
10. Friston, K.J., Daunizeau, J., Kiebel, S.: Action and behavior: a free-energy formulation. Biological cybernetics **102(3)**, 227–260 (2010)
11. Friston, K.J., Mattout, J., Kilner, J.: Action understanding and active inference. Biological cybernetics **104(1-2)**, 137–160 (2011)

12. Khalil, H.K.: High-gain observers in nonlinear feedback control. In: 2008 International Conference on Control, Automation and Systems (2008)
13. van de Laar, T., Özçelikkale, A., Wymeersch, H.: Application of the free energy principle to estimation and control. arXiv preprint arXiv:1910.09823 (2019)
14. van de Laar, T.W., de Vries, B.: Simulating active inference processes by message passing. Frontiers in Robotics and AI **6**(20) (2019)
15. Lanillos, P., Cheng, G.: Active inference with function learning for robot body perception. In: International Workshop on Continual Unsupervised Sensorimotor Learning (ICDL-Epirob) (2018)
16. Lanillos, P., Cheng, G.: Adaptive robot body learning and estimation through predictive coding. In: IROS (2018)
17. Narendra, K.S., Balakrishnan, J.: Adaptive control using multiple models. IEEE Transaction on Automatic Control (1997)
18. Oliver, G., Lanillos, P., Cheng, G.: Active inference body perception and action for humanoid robots. arXiv preprint arXiv:1906.03022v2 (2019)
19. Paviglianiti, G., Pierri, F., Caccavale, F., Mattei, M.: Robust fault detection and isolation for proprioceptive sensors of robot manipulators. Mechatronics **20(1)**, 162–170 (2010)
20. Pezzato, C., Ferrari, R., Corbato, C.H.: A novel adaptive controller for robot manipulators based on active inference. IEEE Robotics and Automation Letters (2020)
21. Pio-Lopez, L., Nizard, A., Friston, K., Pezzulo, G.: Active inference and robot control: a case study. Journal of The Royal Society Interface **13(122)** (2016)
22. Sancaktar, C., Lanillos, P.: End-to-end pixel-based deep active inference for body perception and action. arXiv preprint arXiv:2001.05847 (2019)
23. Van, M., Wu, D., Ge, S., Ren, H.: Fault diagnosis in image-based visual servoing with eye-in-hand configurations using Kalman filter. IEEE Transactions Industrial Electronics **12(6)**, 1998–2007 (2016)
24. Vanderbroeck, M., Baioumy, M., van der Lans, D., de Rooij, R., van der Werf, T.: Active inference for robot control: A factor graph approach. Student Undergraduate Research E-journal! **5**, 1–5 (2019)
25. Zhang, Y., Jiang, J.: Bibliographical review on reconfigurable fault-tolerant control systems. Annual Reviews in Control **32**(2), 229 – 252 (2008)